Journal of Electronics and Sensors
Review Article

A carbon ink screen-printed immunoelectrode for Dengue virus NS1protein detection based on photosynthesized amine gold nanoparticles

Ana C. M. Silva[1], Jamil Saade[1], Ma. Izabel F. Guedes[2], Marli T. Cordeiro[3], Rosa F. Dutra*[1]

[1]Laboratory of Biomedical Engineering, Department of Biomedical Engineering, Federal University of Pernambuco, Recife, Brazil
[2]Human Genetic Laboratory, State University of Ceara, Fortaleza, Brazil
[3]Aggeu Magalhães Research Center, FIOCRUZ-PE, Recife, Brazil

Recevied: 23 April 2018**; Accepted:** 28 May 2018**; Published:** 01 June 2018

***Corresponding Author**: Dutra RF, Laboratory of Biomedical Engineering, Department of Biomedical Engineering, Federal University of Pernambuco, Recife, Brazil.
E-mail: rosa.dutra@ufpe.br

Abstract

Dengue virus (DENV) is a reemerging mosquito-borne disease that is endemic in more than 125 countries, affecting 200 million people per year. Screening testing has been a good attempt to minimize the impact caused by high morbity and mortality rates of DENV. In this study, a simple and disposable label-free electrochemical immunosensor based on a carbon ink graphite screen-printed electrode (SPE) one-step fabricated was developed for detection of non-structural 1 protein (NS1). The SPE surface was modified by drop casting, depositing a colloidal suspension containing amine-functionalized gold nanoparticles (AuNP-NH2). AuNPs were synthetized by a photoinduced physical method, illuminating preformed gold seeds with a light-emitting diode (LED,) at blue region, by using the polyethyleneimine (NH2) as reductor and stabilizing agent. UV-VIS spectroscopy and Transmission Electron Microscopy (TEM) were used to characterize the amine AuNPs. Electrocatalytic activity of AuNPs allowed more sensitivity for a label-free detection of NS1 by square wave voltammetry (SWV), with linear response from 0.1 to 2 µg mL-1. It was found a good linearity (coefficient of correlation of 0.995 ($p<0.01$) and a limit of detection of 0.03 µg mL-1 NS1 for analytical responses. AuNP-NH2 synthesis provided an easy oriented immobilization of

anti-NS1 antibodies by Fc portion, resulting in a simple fabrication immunosensor with relative high performance and feasibility for early diagnostic of DENV.

Highlights

A Dengue electrochemical immunosensor for NS1 label-free detection was developed

Growing of gold nanoparticle (NH2-AuNP) was LED size-controlled

NH2-AuNP increased the electroactive sensor area and immobilized anti-NS1

Analytical response from 0.1 to 2.0µg/mL of NS1 was obtained

It was obtained a simple and easy preparation platform for dengue acute phase.

Keywords: Dengue; Immunosensor; Gold Nanoparticle; NS1; LED Irradiation Synthesis.

Introduction

Dengue is a viral infection considered one of the most important emerging pathogens transmitted by the *Aedes aegypti* and *Aedes albopictus* mosquitoes to human [1]. The year 2016 was characterized by large dengue outbreaks worldwide, affecting mainly the regions of the Americas where was reported more than 2.38 million cases, in which only the Brazil contributed slightly less than 1.5 million cases [2]. Dengue Shock syndrome has been responsible for more than 9000 deaths in 2013 [3]. This number may be higher because there are many cases of asymptomatic patients and under-notification due to the lack of an accurate diagnosis. Early diagnostic of dengue virus (DENV) infection can improve clinical outcomes by ensuring close follow-up, initiating appropriate supportive therapies and raising awareness to the potential of hemorrhage or shock. Non-structural protein 1 (NS1) is a 48-kDa glycoprotein that has proven to be a powerful biomarker for early diagnosis of dengue [4].

A number of rapid diagnostic tests (RDTs) and enzyme-linked immunosorbent assays (ELISAs) targeting NS1 antigen (Ag) are now commercially available [5, 6]. ELISA test is a laboratorial test, requiring personal skilled and are time-consuming. Rapid diagnostic tests (RDTs) based on lateral flow immunoassay has been proposed for NS1 detection as good and practical alternative, however they present some drawbacks related to sensitivity and limited to yes/no responses. RDTs can differentiate the stages of disease according to serum levels of protein in the bloodstream.

Conversely, biosensors can offer quantitative responses through a transducer that converts biochemical reactions in an electrical measurable signal [7]. Different transducers are used, and electrochemical transducers have been more appreciated, mostly the screen-printed electrodes (SPE) that present advantages of easy mass-

production [8]. SPEs are lower cost and more practice compared to electrochemical conventional electrodes, deserving to be emphasized that are discarded after the use, being ideal for biological sample analyses [9,10]. The SPE have been fabricated using a variety of carbon inks with different conductive properties, which can be altered with addition conductive adjuvants, as carbon nanotubes or other allotropes, or even solvent and ionic liquids[11]. Electrochemical biosensors for NS1 have been proposed by our group[12,13] and other authors[3,14]; however, several challenges need to be still achieved, as well an easier of scale up production including an one-step sensor fabrication and a practical read-out measurements.

Gold nanoparticle (AuNP) is an easy-prepared nanomaterial that have been widely employed for biosensors. AuNP exhibits unique and interesting physical, optical and electrochemical properties that hold as a promising potential for biosensor development, offering suitable platforms for protein immobilizations[15]. Depending of synthesis, AuNPs can exhibit electro catalytic activity and improve the electron transfer rate between the electrolyte and electrode surface, being interesting to biosensor preparations [9,16]. Because of their large surface area to volume ratio, gold nanoparticles drop casted on the electrodes retain a greater amount of biomolecules on the sensor surfaces, resulting in a more improved analytical sensitivity [17].

The immobilization way of antibodies or antigens on electrode surface is crucial step to delimit the performance of an immunosensor. Oriented antibody immobilization strategies allowing the Fab portions free to antigen binding are especially important for immunosensing applications, enhancing their analytical responses [18,19]. Amine groups are considered interesting bindings to Fc portion of antibodies, due to simple amide bond formations[20]. To immobilize antibodies as irreversible mode, chemical modifications of AuNPs are necessary[21]. Polyethyleneimine (PEI) is a cationic polymer very stable in aqueous solution, highly branched with high charge density, which contains primary, secondary and tertiary amine groups. PEI is a commonly used stabilizer of gold colloids and many applications of PEI are facilitated by its ability to form complexes with both anionic polyelectrolytes and metal ions. It has been used both as the shape-directing agent to control the preferential growth of crystal seeds in preparation of several shapes so as stabilizing agent[16]. Several primary amine present on branched PEI result in catalytic AuNPs[22]. Another advantage of using PEI is to achieve functional groups on the

nanoparticles surface in only one stage of the one-spot synthesis.

Herein, an innovative label-free electrochemical immunosensor using amine gold nanoparticles (AuNP-NH_2) is proposed for NS1 protein detection of dengue virus. AuNPs were amine functionalized, to orientate antibodies by Fc portions on the electrode surface, whereas as also is guaranteed more stable sensing platforms. This approach is an struggling to demonstrate that immunosensing devices employing simple functionalized AuNP can be developed, in order to aid several disease diagnostics.

Materials and Methods

Materials and reagents

The carbon ink screen printed electrodes (SPE) were fabricated according to our previous work[23], which contained the Electrodag PF-407 C carbon ink and graphite powder acquired from acquired from Acheson Henkel and Fluka, respectively. Polyethyleneimine (PEI, branched, Mw 10,000), chloroauric acid ($HAuCl_4$), N-hydroxysuccinimide (NHS) and N-ethyl-N′-(3-dimethylaminopropyl) carbodiimide (EDC) were obtained from Sigma-Aldrich (United States). Dengue virus NS1 glycoprotein 480 nm and 10 watts power. It was observed that the solutions turned into a pale red color after exposure to LED for 6 h. The color of the (>90% purity) and mouse monoclonal antibodies against dengue virus NS1 glycoprotein (anti-NS1) were purchased from Abcam (United Kingdom). All other reagents used for buffer and solution preparation were of analytical grade. Ultrapure water (18.2 MΩ cm) was obtained from a Milli-Q water purification system (Millipore Inc., United States).The culture supernatant with NS1 native protein was grown from DENV-3 (strain 101.905/BR-PE/03) and collected 5th day after inoculation in C6/36 cell monolayers, maintained in Leibovitz L-15 medium (GIBCO, Invitrogen, Grand Island, NY) containing 2% fetal calf serum. NS1 in culture supernatant was confirmed and quantified by in house ELISA, employing an anti-NS1 monoclonal antibody[24]. As control cell, it was used C6/36 supernatant cell culture (without virus infection) collected at 5th day. Both supernatants were cleared by centrifugation for 10 min at 1.500 rpm (400 g).

Synthesis of PEI-AuNPs

PEI (1.45 g) was dissolved in 5 mL Milli-Q water and then mixed to 3 mL of $HauCl_4$ (1.1 mmol L^{-1}) to form a homogeneous solution. Afterwards, the solution was exposed to Light Emission Diode (LED) at reaction mixture would gradually deepen with the increase of exposure time. During the reduction of Au (III) metal ions through amine groups of the PEI, it acted as an agent

for multiple functions: stabilizer, shape-controller of gold nanoparticles and as a weak reductant

Figure (1(a)): AuNP-NH_2 synthesis

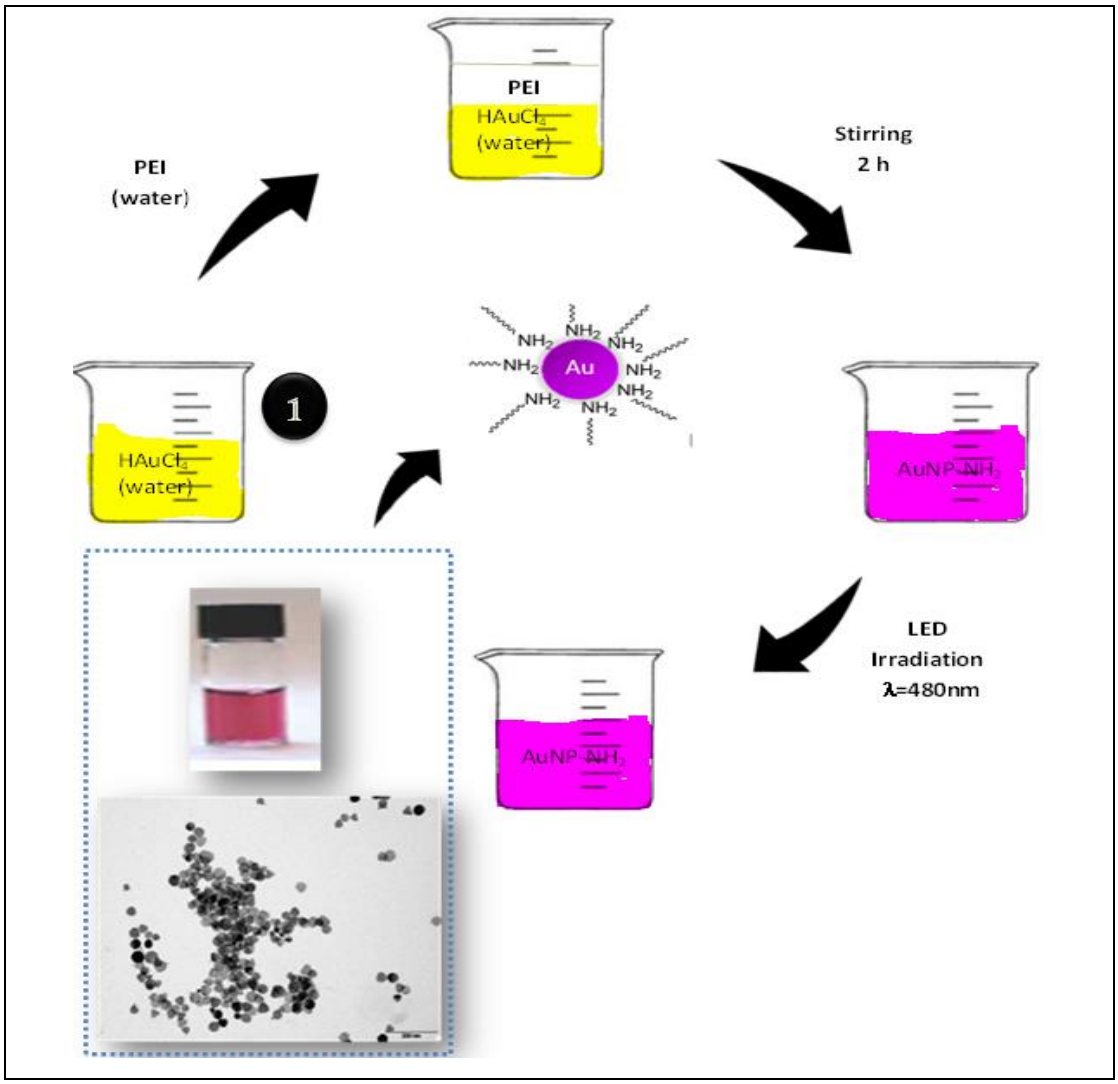

Preparation of immunoelectrode and immunoassay

The SPE was home-made fabricated and polished according to previously described[23]. The PEI-AuNP layer on the electrode surface were obtained by drop casting method, by applying one layer of 10 µL. Afterwards, 10 µL of anti-NS1 antibodies solution (10 µg mL^{-1}) diluted in solution of 50mM NHS and 20 mM EDC [1:1] in 0.1 citrate phosphate buffer (pH 6.5) was incubated on the SPE surface for 2 h at room temperature. After two PBS washes, non-specific bindings were blocked by incubating the modified electrode surface in a 0.05 mol L^{-1} glycine solution prepared in PBS (pH 7.4)

for 2 h, at room temperature. Excess of non-bound glycine were removed by PBS washes.

Analytical responses of the immunosensor were evaluated by incubating the anti-NS1 sensor surface with 10 µL of NS1 samples in different concentrations. This procedures were performed at 30 min incubation time, in a moist chamber at room temperature. Different incubation times were previously tested, showing responses after 10 min, however up to 30 min the maximal response was obtained.

Figure (1(b)): Preparation of the immunoelectrode.

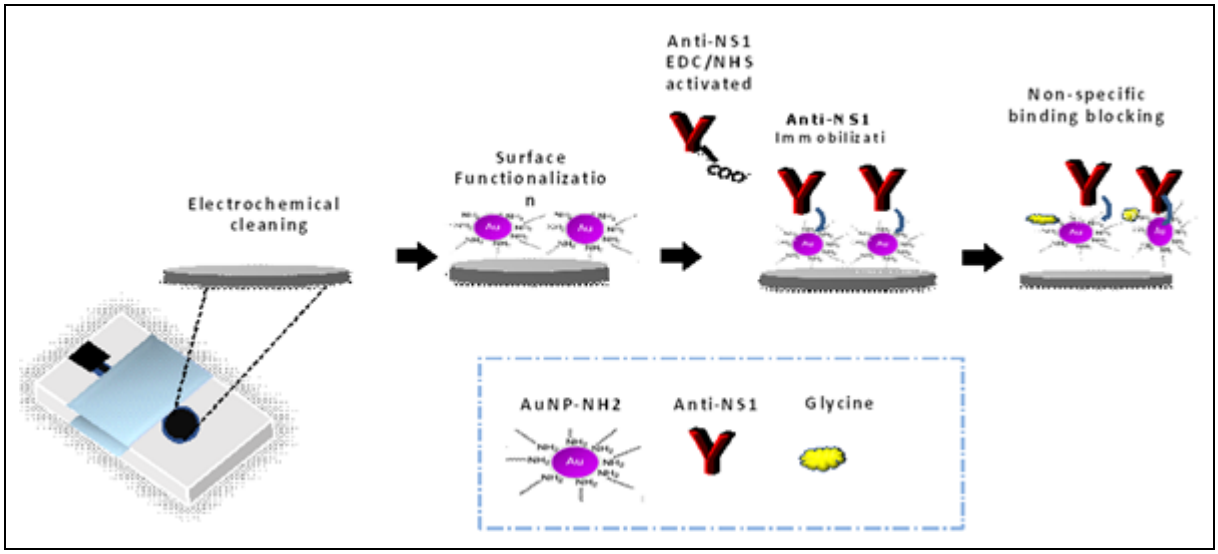

Electrochemical characterization and analytical responses

All electrochemical measurements were performed in an Ivium Compact Stat potentiostat/galvanostat from Ivium Technologies (Netherlands), interfaced with a microcomputer and controlled by Ivium Soft software. A three-electrode electrochemical cell used consisted of the SPE as working electrode, an Ag/AgCl electrode as reference electrode and a helical platinum wire as counter electrode. The experiments to characterize the assembling of the SPE were carried out in the electrochemical cell by cyclic voltammetry in 0.005 mol L^{-1} $K_3Fe(CN)_6/K_4Fe(CN)_6$ prepared in 0.1 mol L^{-1} KCl solution, at 0.05 V s^{-1} scan rate and potential ranging from -0.6 to 1.0 V vs. Ag/AgCl (3 mol L^{-1} KCl).

Immunosensor responses were generated by square wave voltammetry (SWV) monitored at potential range from -0.2 to 0.7 V, frequency of 10 Hz and pulse amplitude of 10 mV. The responses were obtained from current differences from blank (after glycine blocking) and after the NS1 incubation step. The relative current was calculated dividing to blank in order to

normalize the differences between the electrodes.

Figure (1(c)): Graphical Abstract

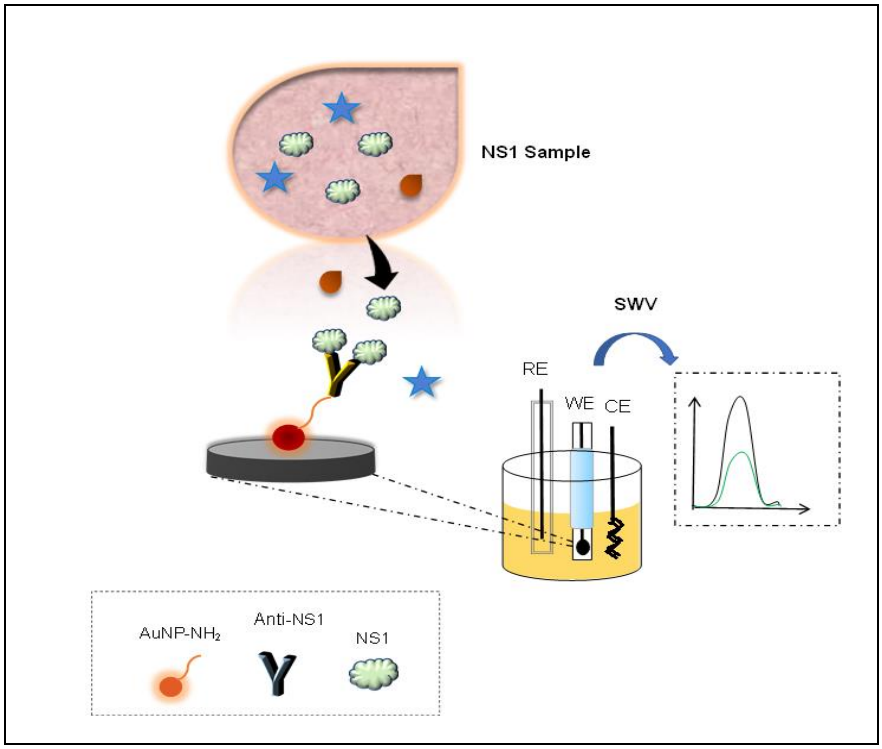

PEI AuNPs characterization

AuNPs colloids were characterized by UV–Vis Spectroscopy (Bruker Spectrophotometer UV-vis 3000). The morphology of AuNPs was analyzed by a Transmission Electron Microscopy (TEM), using a FEI Tecnai20 operating at 200 kV. Chemical composition of PEI-AuNPs nanocomposite was investigated by Energy-Dispersive X-ray spectroscopy (EDX), integrated to a FEI Quanta 200 FEG microscope (Netherlands). Fourier transform infrared (FTIR) spectroscopy was performed to chemically characterize the electrode surface. FTIR measurements were performed in attenuated total reflectance (ATR) mode using a Vertex 70 FTIR (scans=64, energy scanning from 400 cm^{-1} to 4000 cm^{-1}), acquired from Bruker (Germany).

Results and Discussion

Characterization of NH_2-AuNPs

Chemical structure characterization of PEI-AuNP was performed by UV-VIS analysis. Spectrum absorption band modifications in the visible or near-infrared wavelength region are influenced by the dielectric environment of the surface of the nanoparticles. These changings are attributed to the localized surface Plasmon resonance (LSPR) phenomenon that occurs in Nano-

sized due to the electronic oscillation on the metal nanoparticle surface[25].

During the initial stage of growth of colloid, the solution exhibited a light yellow color and only one intense adsorption band attributed to the ligand-metal charge-transfer band of the gold salt was observed at ultraviolet, 300 nm in the left band[26]. However, increasing the exposure time, the solution became reddish and the extinction spectrum showed two additional absorption bands: one placed at 530 nm with a good symmetry, assigned to the in-plane dipole resonance of polyhedral nanoparticles[21,27] and, a much weaker small band around 370 nm that can be attributed to the interband electronic transitions of gold in articles **(Figure 2(a)**).

The prominent band at 530 nm is attributed to the LSPR band of the PEI-AuNPs. Its location is related to the average size of particle and its width to the standard deviation. The refraction index od solvent and presence of the PEI also influences the LSPR band[28], but the biggest change occurs with inter-particle distance. In this case, the aggregation of NPs leaded to a pronounced color change as a consequence of the plasmon coupling between NPs and a concomitant red-shift of the LSPR absorption band peak [29]. Location of this band for particles dispersed in water, without any molecule adsorbed on its surface is around 520 to 530 nm and represents, typically, that the synthetized golf nanoparticles have a diameter from 5 to 100 nm.

In order to confirm the size distribution of the PEI-AuNPs, a TEM was performed (Figure (2(b)). According to histogram (inset Figure 2(b)), the size distribution of PEI-AuNP were normally distributed with range from 4 to 14 nm diameter (95% IC) with an average diameter of 9.5 ± (1.1) nm. This short variation in size is results of a controlled synthesis done by LED irradiation, moreover the size is also dependent of polymer chemical precursor [30]. Herein, the use of a branched PEI with medium size chain allowed non-significant variation. A non-regular size of nanoparticles can results in a non-regular and prominent current peaks compromising the electrochemical responses [31].

Figure (2): AuNP-NH_2 characterization In (a) Extinction spectrum and (b) TEM micrograph Inset represents the nanoparticles histogram with approximately 200AnNPs.

2(a) Extinction spectrum

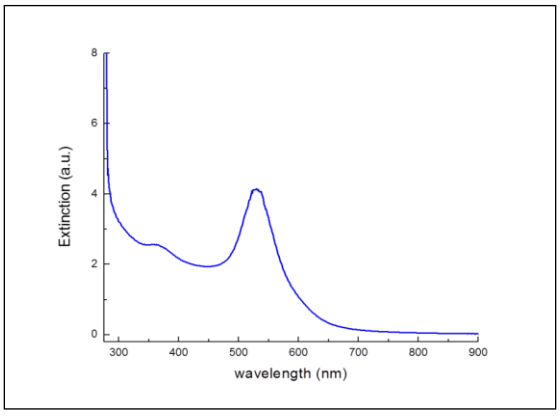

2(b) TEM micrography

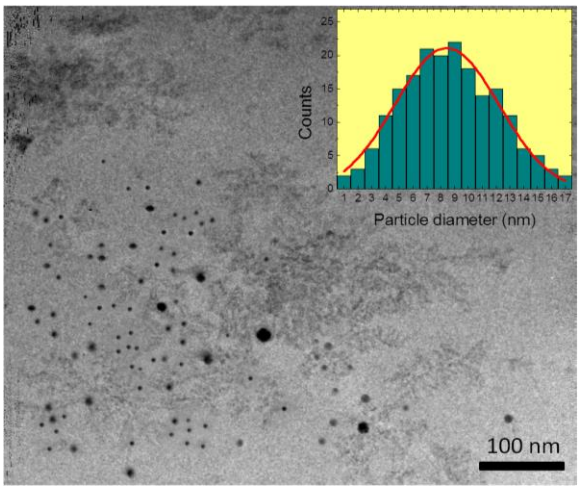

Characterization of SPE surface modified by NH_2 AuNPs

The EDX analysis shows the elemental composition of the electrode surface before and after modification. **Figure 3(a)** shows EDX spectra of the bare SPE (a) and SPE modified with NH2-AuNPs (b). Bands corresponding to C, O and Cl elements were observed on the spectrum. These elements are carbon ink components used in the fabrication of the SPE. In **Figure 3(b)**, it was observed an Au peak, confirming that the AuNPs recovered the SPE surface. The Cr peak is due to thin conductive coating applied to enable SEM investigation. FTIR spectra were also used to investigate the modification of the SPE with NH2-AuNPs. The FTIR spectra.

The fundamental vibrations in the 4000–2500 cm^{-1} region are generally due to O–H, C–H and N–H stretching. O–H stretching produces a broad band that occurs in the range 3700–3600 cm^{-1}. By comparison, N–H stretching is usually observed between 3400 and 3300 cm^{-1} [32]. The curve (a) shows clean SPE spectrum that presents a characteristic band at 3411 cm^{-1} corresponding to O-H molecular stretching. On the other hand, the curve (b), after electrode surface modification with NH2-AuNPs, showed the band of N–H stretching at 3281 cm^{-1} confirming the presence of the polymer on the SPE surface. It is also possible see at the spectrum (b) bands at 1634 cm^{-1} and 1471 cm^{-1} that are associated to N–H asymmetric bending and C–H stretch [33].

Figure (3): EDX spectra

3(a) bare SPE

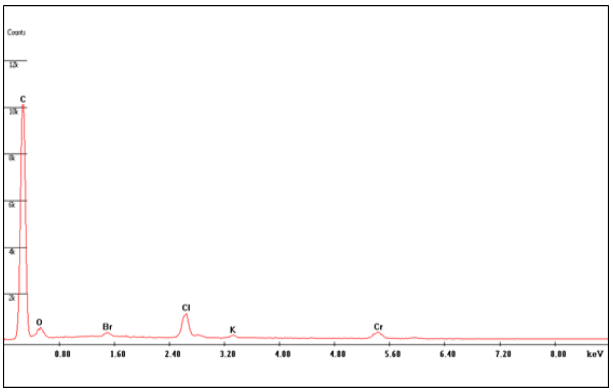

3(b) SPE of the AuNP-NH_2

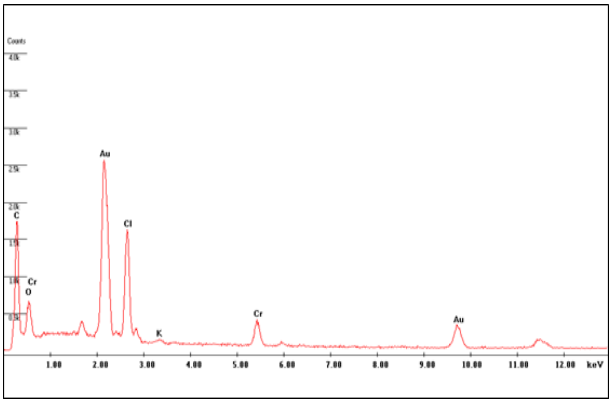

Figure (4): FTIR spectra in ATR mode: (a) bare SPE and (b) AuNP-NH_2 /SPE.

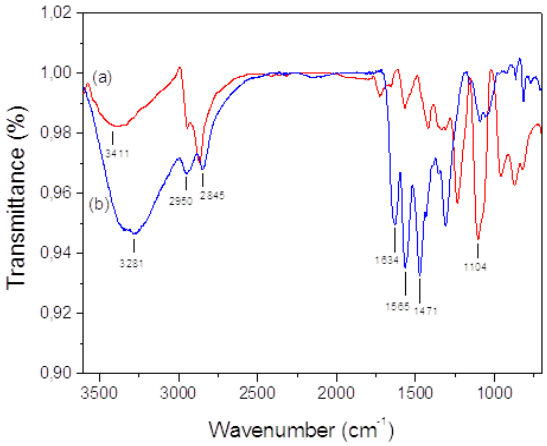

Electrochemical characterization

Cyclic voltammetry is an effective method to electrochemically characterize the modified electrode surface. This technique clearly shows that the dynamics of charge transfer at the electrochemical interface is strongly influenced by the nature of the electrode surface and also by the structure of the electric double layer [34]. Each assembly step of the modified electrode was electrochemically characterized using 0.005 mol L^{-1} $K_3Fe(CN)_6/K_4Fe(CN)_6$ as redox probe. A well-defined and reversible redox peaks were observed on the bare SPE (curve a). An increase in amperometric response was observed after NH_2-AuNPs deposition (curve b). This increase of electroative area confirm the deposition of the NH_2-AuNP formation, as also mentioned [35]. NH_2-AuNPs Nano composites were incorporated to the sensor platform, enhancing the electron transfer and facilitating the electron exchange between the electrode surface due to their catalytic proprieties. SPE surface modification with NH_2-AuNPs resulted in an increase of approximately 78 ± 3% and 67 ± 4%. Percentage in anodic and cathodic current peaks, respectively for three replicates analyses. A major amplitude in anodic peak is justified by amine groups present in AuNp. A decrease of the amperometric response was also observed after the immobilization of the anti-NS1 antibodies and blocking with glycine (curves c and d). This decrease occurred because the anti-NS1 antibodies are biomolecules of insulating nature, increasing the diffusion barrier [7, 36]. Analytical immunosensor response is highly dependent of immobilized antibodies and the antigen binding capacity[20]. In this work, NH2 polymer was used to promote a covalent immobilization of the anti-NS1 antibodies via amide bonds. For this, the Fc terminal of the anti-NS1 antibodies was activated by EDC/NHS mixing. The oriented immobilization of antibodies by Fc portion enhances the sensitivity and selectivity of the immunosensor through the exposing of the Fab portions, which have a high affinity for the antigens [37]. In order to improve the immunoassay sensitivity, the anti-NS1 concentration immobilized on the sensor surface was optimized. Different concentrations of anti-NS1 (from 0.5 to 20 µg mL^{-1}) prepared in PBS were immobilized on

the SPE surface. The immunosensor response showed a maximal concentration at 10g mL^{-1} anti-NS1 **(Figure 5(b)).** Therefore, this concentration was chosen for the remaining experiments.

Figure (5(a): Cyclic voltammograms of the immunosensor in each step of immobilization: (curve a) bare SPE; (curve b) NH_2-AuNPs/SPE; (curve c) anti-NS_1/NH_2-AuNPs/SPE and (curve d) glycine/anti-NS1/ AuNP-NH_2 /SPE. Scans performed in 0.005 mol L^{-1} $K_3Fe(CN)_6/K_4Fe(CN)_6$, at 0.05 V s-1 scan rate.

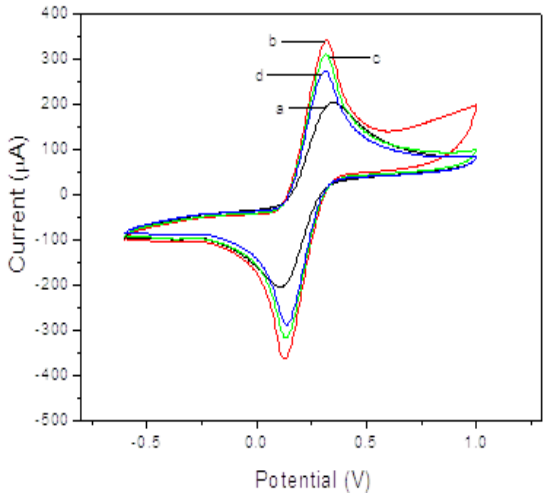

Figure (5(b)): Effect of Anti-NS1 concentration immobilized on the electrode surface against the NS1 response.

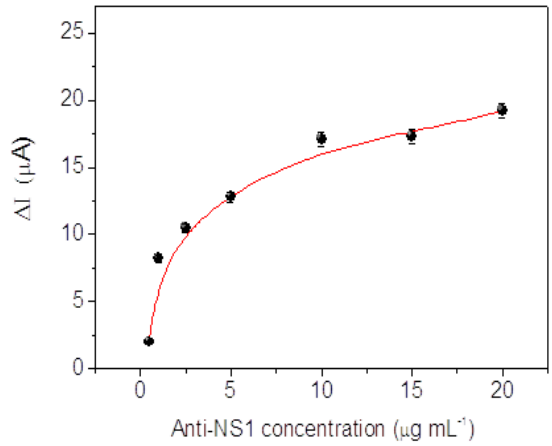

Stability of NH_2-AuNPs film

The stability of the PEI-AuNPs film on the SPE surface was evaluated by 15 successive cyclic voltammograms of the PEI-AuNPs/SPE performed in presence of 0.005 mol L^{-1} of $K_3Fe(CN)_6/K_4Fe(CN)_6$, prepared in 0.1 mol L^{-1} KCl, at 0.05 V s^{-1} scan rate and at potential ranging from -0.6 to 1.0 V. After 15 cycles, the redox peaks were practically constant. It was obtained a coefficient of variation (CV) of approximately 2%, to anodic peak, and 3%, to cathodic peak **(Figure 6(a))**, indicating a good stability of the film on the SPE surface (CV < 5%).

Figure (6(a)): Typical cyclic voltammogram representative of stability of NH2-AuNPs film at 20 cycles.

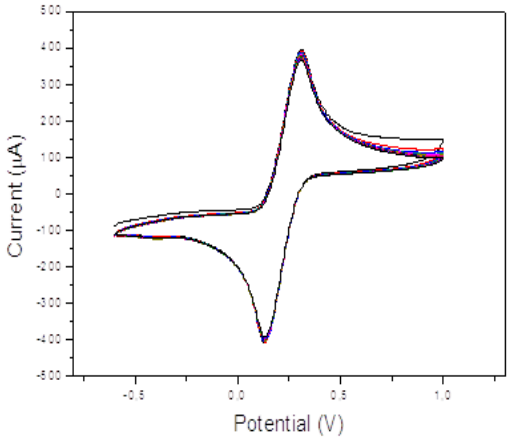

Figure (6(b)): Analytical response as function of incubation time.

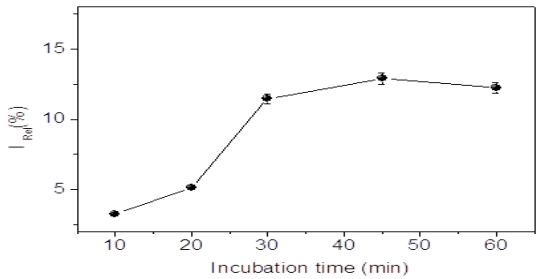

Incubation time of antigen-antibody influences on the immunosensor response. Commonly it changes from 15 to 60 min. An optimal incubation time promotes a maximal binding capacity responses [38]. Thereby, the effect of incubation time of NS1 antigen on the response immunosensor was also evaluated. Anti-NS1/NH2-AuNPs/SPE was incubated with NS1 antigen (1 µg/mL) during periods from 10 to 60 min. The incubation time reached the maximum at 30 min and became stable when the time was exceeded, indicating the interaction between NS1 antigen and anti-NS1 antibody.

Analytical response of the immunosensor:

The calibration curve was performed in different NS1 concentrations by using SWV, in a solution of $K_3Fe(CN)_6/K_4Fe(CN)_6$ (0.005 mol L^{-1}) prepared in 0.1 mol L^{-1} KCl, at 0.05 V s^{-1} scan rate. The immunosensor was incubated with successive NS1 samples, under optimized experimental conditions, in the range of concentration of 0.1 to 2.0 µg mL^{-1}, diluted in PBS solution (0.01 mol L^{-1}, pH 7.4). The results showed a decrease of the peak current proportional to the increase of NS1 concentration (Figure 7a). A linear calibration curve was obtained in the concentration range from 0.1 to 2.0 µg. mL^{-1} NS1 with a correlation coefficient of 0.99515 ($p < 0.0001$, $n = 7$) and the sensitivity of immunosensor was approximately 5.6 µA/µg.mL^{-1} NS1. The calculated limit of detection (LOD = three times the standard deviation of the intercept/slope) was found at 0.09 µg mL^{-1}. A report by Alcon et al. (2002) [39] demonstrated that serum levels of NS1 antigen in primary and secondary infections by DENV1 were found in the range from 10 ng mL^{-1} to 2 µg mL^{-1}. It was also detected elevated levels of free secreted NS1 (≥ 600 ng mL^{-1}) in patients on the illness onset, at risk for developing dengue hemorrhagic fever [40]. This clinical range for NS1 protein match with values detected by this immunosensor. The reproducibility of the immunosensor was also investigated by performing SWV measurements in $K_3Fe(CN)_6/K_4Fe(CN)_6$ (0.005 mol L^{-1}) prepared in 0.1 mol L^{-1} KCl , at 0.05 V s^{-1} scan rate. The analytical response of 8 different electrodes prepared under the same conditions was evaluated. For this, the electrodes were incubated with 1 µg mL^{-1} NS1 protein during 30 min. Coefficient of variation of 4.3% was achieved, indicating a good reproducibility of the immunosensor. Taking account that the anti-NS1 used was produced by a recombinant antigen, the specificity on responses were evaluated against native NS1 antigens. In this assay, virus dengue isolated from serum samples of four serotypes were grown and samples collected in the 5th day, after inoculation in C6/36 cell monolayers, period established for a maximal NS1

expression. According to bar plot exhibited. Immunosensor showed a positive response to the four serotypes of DENV. It was also observed in NS1 serotype 3, a lower current response in comparison to 1, 2 and 4 serotypes, that can be attributed to a lower viremy of DENV3. In addition, the specificity was checked against C6/36 control cells grown without any DENV inoculation and, the amperomentrical immunosensor response was practically null current, demonstrating a good selectivity of this analytical method.

Figure (7(a)): Analytical curve of NS1 immunosensor; Inset: SWVs of analytical responses to NS1

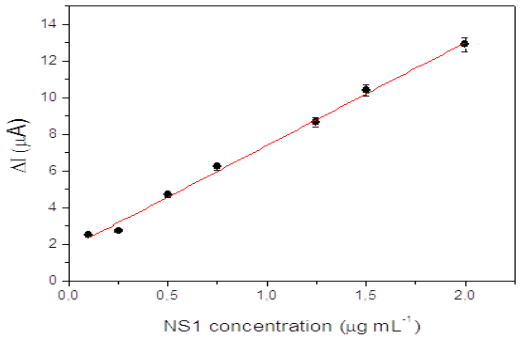

Figure (7(b)): Immunosensor responses to native antigens against supernatant cultures of four serotypes. Measurements performed in 0.005 mol L-1 $K_3Fe(CN)_6/K_4Fe(CN)_6$, at 0.05 V s-1 scan rate.

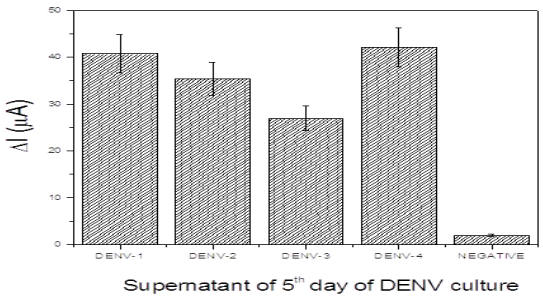

Conclusions

An electrochemical immunosensor was successfully developed for NS1 protein DENV detection. NH_2 AuNP synthetized by branched PEI with longer chain resulted in metallic nanoparticle with a good catalytic activity, improving the electrochemical response. This approach is a point-of-care attempting to prevent the acute phase, with early diagnostic. The fabrication procedure of tip sensor is simple and based on one-step synthesis of amine functionalized gold nanoparticle. NS1 levels is found a clinical range, and this biosensor was capable to detect the four serotype of dengue virus.

Acknowledgements

The authors are grateful the National Council of Scientific and Technological Development (CNPq) and ACM Silva thanks to Foundation of Support to Science and Technology of the State of Pernambuco (FACEPE) for scholarship during this work.

Reference

1. Smartt CT, Shin D, Alto BW (2017) Dengue serotype-specific immune response in Aedes aegypti and Aedes albopictus, Mem. Inst. Oswaldo Cruz; 112(12): 829-837.
2. Weekly epidemiological record Relevé épidémiologique hebdomadaire; 91(2016): 349-364.
3. Cecchetto J, Carvalho FC, Santos A et al. (2015) An impedimetric biosensor

to test neat serum for dengue diagnosis; 213: 150-154.

4. Datta S, Chatterjee S, Veer V (2014) Recent advances in molecular diagnostics of hepatitis B virus, World J. Gastroenterol; 20(40).
5. Pal S, Dauner AL, Mitra I et al. (2014) Evaluation of dengue NS1 antigen rapid tests and ELISA kits using clinical samples. PLoS One; 9(11).
6. Hunsperger EA, Yoksan S, Buchy Pet al. (2014) Evaluation of commercially available diagnostic tests for the detection of dengue virus NS1 antigen and anti-dengue virus IgM antibody. PLoS Negl. Trop. Dis; 8(10).
7. Silva MMS, Dias ACMS, Silva BVM et al. (2015) Electrochemical detection of dengue virus NS1 protein with a poly(allylamine)/carbon nanotube layered immunoelectrode. J. Chem. Technol. Biotechnol; 90(1):194-200.
8. Gornall DD, Collyer SD, Higson SPJ (2009) Investigations into the use of screen-printed carbon electrodes as templates for electrochemical sensors and sonochemically fabricated microelectrode arrays. Sensors Actuators. B Chem; 141(2): 581-591.
9. Cao X, Ye Y, Liu S (2011) Gold nanoparticle-based signal amplification for biosensing. Anal. Biochem; 417(1):1-16.
10. Trojanowicz M (2016) Impact of nanotechnology on design of advanced screen-printed electrodes for different analytical applications, TrAC Trends Anal. Chem; 84: 22-47.
11. Fanjul-Bolado P, Hernández-Santos D, Lamas-Ardisana Pj, et al. (2008) Electrochemical characterization of screen-printed and conventional carbon paste electrodes. Electrochim. Acta; 53(10): 3635-3642.
12. Silva MMS, Dias ACMS, Cordeiro MT, et al. (2014) A thiophene-modified screen printed electrode for detection of dengue virus NS1 protein, Talanta; 128: 505-510.
13. Dias ACMS, Gomes-Filho SLR, Silva MMS, et al. (2013) A sensor tip based on carbon nanotube-ink printed electrode for the dengue virus NS1 protein. Biosens. Bioelectron; 44: 216-221.
14. Darwish NT, Alrawi AH, Sekaran SD, et al. (2016) Electrochemical Immunosensor Based on Antibody-Nanoparticle Hybrid for Specific Detection of the Dengue Virus NS1 Biomarker. J. Electrochem. Soc; 163(3): B19-B25.
15. Alkilany AM, Murphy CJ (2010) Toxicity and cellular uptake of gold nanoparticles: what we have learned so far?. J. Nanoparticle Res.; 12(7): 2313-2333.
16. Saha K, Agasti SS, Kim C, et al. (2012) Gold Nanoparticles in Chemical and Biological Sensing, Chem. Rev; 112(5): 2739-2779.
17. Brondani D, de Souza B, B. Souza S, et al. (2013) PEI-coated gold nanoparticles decorated with laccase: a new platform for direct electrochemistry of enzymes and biosensing applications. Biosens. Bioelectron; 42: 242-247.
18. Baniukevic J, Kirlyte J, Ramanavicius A, et al. (2012) Comparison of Oriented and Random Antibody Immobilization Techniques on the Efficiency of Immunosensor. Procedia Eng; 47: 837-840.

19. Duval F, van Beek TA, Zuilhof H (2015) Key steps towards the oriented immobilization of antibodies using boronic acids. Analyst; 140(19): 6467-72.
20. Pei Z, Anderson H, Myrskog A, et al. (2010) Optimizing immobilization on two-dimensional carboxyl surface: pH dependence of antibody orientation and antigen binding capacity. Anal. Biochem; 398(2): 161-168.
21. Wu HL, Kuo CH, Huang MH (2010) Seed-Mediated Synthesis of Gold Nanocrystals with Systematic Shape Evolution from Cubic to Trisoctahedral and Rhombic Dodecahedral Structures. Langmuir; 26(14): 12307-12313.
22. Dong H, Dai Y, Zhang X, et al. (2018) The influence of amine structures on the stability and catalytic activity of gold nanoparticles stabilized by amine-modified hyperbranched polymers. Nanotechnology; 29(5): 55705.
23. Dias ACMS, Gomes-Filho SLR, Silva MMS, et al. (2013) A sensor tip based on carbon nanotube-ink printed electrode for the dengue virus NS1 protein. Biosens. Bioelectron; 44: 216-221.
24. Cordeiro MT (2012) Laboratory diagnosis for dengue. Rev. Inst. Med. Trop. Sao Paulo; 54: 10-12.
25. Park JH, Byun JY, Yim SY, et al. (2016) A Localized Surface Plasmon Resonance (LSPR)-based, simple, receptor-free and regeneratable Hg2+ detection system. J. Hazard. Mater; 307: 137-144.
26. I.P.-S. and IPS, Liz-Marzán LM (2002) Formation of PVP-Protected Metal Nanoparticles in DMF; 18(7): 2888-2894.
27. Kim D, Heo J, Kim M, et al. (2009) Size-controlled synthesis of monodisperse gold nanooctahedrons and their surface-enhanced Raman scattering properties. Chem. Phys. Lett; 468(4-6): 245-248.
28. Moores A, Goettmann F (2006) The plasmon band in noble metal nanoparticles: an introduction to theory and applications. New J. Chem; 30: 1121.
29. Jain PK, †El-Sayed MA (2007) Universal Scaling of Plasmon Coupling in Metal Nanostructures: Extension from Particle Pairs to Nanoshells. Nano Lett; 7(9): 2854-2858.
30. Shimmin RG, Schoch AB, Braun PV (2004) Polymer size and concentration effects on the size of gold nanoparticles capped by polymeric thiols. Langmuir; 20(13): 5613-5620.
31. Bonanni A, Pumera M, Miyahara Y (2011) Influence of gold nanoparticle size (2–50 nm) upon its electrochemical behavior: an electrochemical impedance spectroscopic and voltammetric study. Phys. Chem. Chem. Phys.; 13: 4980.
32. Stuart B (2004), Infrared spectroscopy : fundamentals and applications. John Wiley & Sons Ltd;
33. Deng S, Fulghum TM, Krueger G, et al. (2011) Hybrid gold-nanoparticle-cored conjugated thiophene dendrimers: Synthesis, characterization, and energy-transfer studies. Chem. A Eur. J; 17(32): 8929-8940.

34. Kulkarni SA, Mulla IS, Vijayamohanan K (2006) Electrochemical Characterization of Self-Assembled Monolayers on Semiconducting Substrates for MEMS Applications. J. Phys. Conf. Ser; 34: 322-329.
35. Zapp E, Westphal E, Gallardo H, et al. (2014) Liquid crystal and gold nanoparticles applied to electrochemical immunosensor for cardiac biomarker. Biosens. Bioelectron.; 59: 127-133.
36. Zhu Y, Cao Y, Sun X, et al. (2013) Amperometric immunosensor for carbofuran detection based on MWCNTs/GS-PEI-Au and AuNPs-antibody conjugate. Sensors (Basel); 13(4): 5286-5301.
37. Silva BVM, Cavalcanti IT, Silva MMS, et al. (2013) A carbon nanotube screen-printed electrode for label-free detection of the human cardiac troponin T. Talanta; 117: 431-437.
38. Rudmann SV (2005) Textbook of blood banking and transfusion medicine, Elsevier/Saunders;
39. Alcon S, Talarmin A, Debruyne M, et al. (2002) Enzyme-linked immunosorbent assay specific to Dengue virus type 1 nonstructural protein NS1 reveals circulation of the antigen in the blood during the acute phase of disease in patients experiencing primary or secondary infections. J. Clin. Microbiol; 40(2): 376-81.
40. Libraty DH, Young PR, Pickering D, et al. (2002) High Circulating Levels of the Dengue Virus Nonstructural Protein NS1 Early in Dengue Illness Correlate with the Development of Dengue Hemorrhagic Fever. J. Infect. Dis; 186(8): 1165-1168.

***Citation*:** Dutra RF (2018), Silva ACM, Saade J, et al. A carbon ink screen-printed immunoelectrode for Dengue virus NS1protein detection based on photosynthesized amine gold nanoparticles. J Electron Sensors; 1(1): 1-16.

DOI: **10.31829/2689-6958/jes2018-1(1)-102**